Viscoelastic Effects on Wrinkle Formation during Tow Steering in Automated Fiber Placement

Nima Bakhshi, Muhsan Belhaj and Mehdi Hojjati

Concordia Center for Composites, Department of Mechanical, Industrial and Aerospace Engineering, Concordia University, 1455 De Maisonneuve Blvd. W., Montreal, Quebec, H3G1M8, Canada.
Email: nima.bakhshi91@gmail.com

Keywords: Automated Fiber Placement, Tow Steering, Wrinkle, Viscoelasticity.

Abstract
Various defects that appear during tow steering in Automated Fiber Placement, significantly limit the application of this technology while preventing engineers from further optimizing the design of composite materials. This study is focused on the effect of viscoelastic properties that prepreg materials exhibit, on the formation of one of the most predominant process defects, namely wrinkles. Wrinkles appear at the inside edge of the steered tows as a result of local tow buckling. An example of experiments for the case where wrinkles appear with time is presented. A novel buckling model for an orthotropic plate resting on a generalized viscoelastic Pasternak foundation is developed. Furthermore, application of the developed model for wrinkle formation during tow steering is discussed.

1. Introduction

Unique features of the Automated Fiber Placement have led this technology to gain significant importance in the aerospace industry. Differential tow pay-out enables AFP to steer the tows and to laminate complex geometries. In order to keep the desired fiber orientation in complex geometries, steering away from the geodesic path of the mold is inevitable. In addition, the steering ability opens a new, more flexible design space for further tailoring the mechanical behavior of composite structures using curvilinear fiber paths [1].

The formation of various defects during the layup process constrains capabilities of AFP machines including their ability to steer tows. These defects include gaps and overlaps between the courses, out-of-plane wrinkles at the inside edge of the prepreg tow, blisters, etc. [1, 2]. As the tow is laid down onto the tool surface with a prescribed steered path, compressive stress builds up at the inside edge of the tow causing local buckling of the tow and appearance of wrinkles.

Previously, local models [3] and global simulations [4] have been proposed to investigate the formation of wrinkles during the tow steering. However, they both treat the prepreg tow and the prepreg-tool interface (commonly known as tack) with elastic properties. Indeed, it has been pointed out [1] that one possible reason for inconsistencies between the theoretical models and data from AFP experiments is the inability of the models to account for the viscoelastic effects. Prepreg tack which is the main mechanism by which the prepreg is kept onto the tool surface is a product of bulk resin properties as well as the interfacial prepreg-tool properties both of which exhibit time-dependent viscoelastic behavior. In the present study, a novel model accounting for the viscoelastic effects of the interface is suggested. Additionally, an example of experiments for the case where wrinkles appear with time is presented. Furthermore, application of the developed model for wrinkle formation during tow steering is discussed.

2. Model development

During the prepreg deposition process, prepreg materials are transferred from the spools to the compaction roller, through the AFP head's feeding mechanism. The compaction roller incrementally lays down the prepreg onto the surface of the tool, while forcing the prepreg to follow the prescribed trajectory of the AFP head. The application of heat, which is generated for example by a hot gas torch, and compaction force helps in establishing the prepreg tack. As the prepreg is gradually laid down, the compressive stress builds up (induced as a result of the deformation of prepreg tow) in the inner edge of the tow. Once the laid down length is long enough, the stored elastic energy inside the prepreg will be too high for the prepreg tack to keep the prepreg on the tool surface. Therefore, the prepreg tow buckles at its inner edge to drop the excessive amounts of energy stored. The experimental AFP trials confirm that each of these small wrinkles is indeed formed individually with the progress of the deposition process.

Experimental observations, as well as the phenomenological explanation of the wrinkle formation process, suggest that each wrinkle could be analyzed individually and this approach will be utilized in this paper. The presence of unidirectional fibers embedded inside the viscoelastic resin causes the prepregs to have an orthotropic viscoelastic behavior. Meaning that the prepreg's response to stress depends on rate, as well as the load and temperature history. Among different directions, the on-axis fiber direction is least dependent on these parameters, while transverse direction and in-plane shear modulus are dominated by the resin's characteristics. Since the complete load and temperature history of the material are too complex, the prepreg is considered to be a linearly elastic orthotropic plate. This is a reasonable assumption since the stress relaxation effects inside the resin are in favor of having a good, defect-free layup quality.

Prepreg tack is a function of interface properties and bulk properties of the resin. Moreover, the prepreg-tool interface (i.e. prepreg tack) is the primary mechanism resisting against different types of defects occurring in AFP. As the stress relaxation effects take place in the interface, the ability of the tack to keep the steered tow on the tool surface decreases (since elastic modulus decreases), hence facilitating the tow buckling and wrinkle formation process. As mentioned before, it has been suggested that ignoring the viscoelastic effects can be one of the sources of discrepancies between the AFP data and theoretical models. Therefore, contrary to the bulk prepreg material behavior, the time- and rate-dependent viscoelastic effects cannot be ignored in the interface.

Finally, the problem of time-dependent wrinkle growth in steered tows can be formulated as the time-dependent buckling of an elastic orthotropic plate which is resting on a viscoelastic foundation (representing prepreg tack) and is subjected to in-plane loading (Fig. 1).

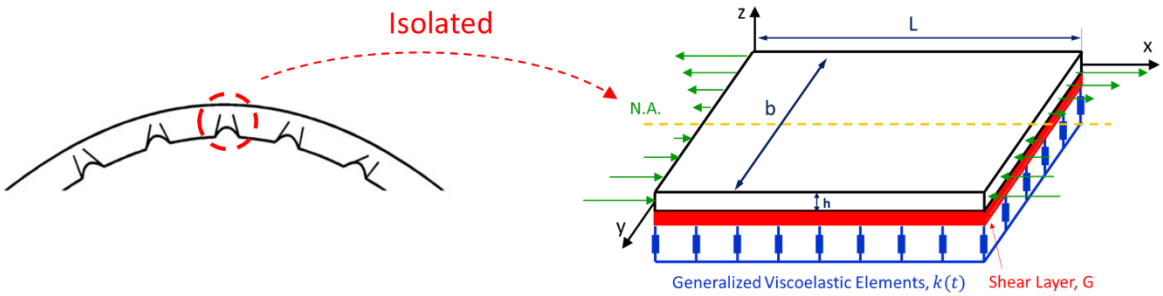

Figure 1. Problem definition.

2.1. Viscoelasticity and buckling

One way for introducing viscoelastic effects into elasticity problems is to add different branches of dashpots (representing a Newtonian flow which has a rate-dependent response) with different configurations to the elastic material representation, which is a Hookean spring (see e.g. [5]). A more general approach would be to use integral constitutive equations of viscoelastic materials stress-strain response. Having the stress relaxation or creep functions, one can use Boltzmann or Stieltjes integral formulae to relate the stress and strain histories in a viscoelastic medium. Review of the available exact and approximate methods for solving the boundary value problems of viscoelasticity is presented in [6]. The latter method is utilized in the present study since it offers a more flexible and general approach.

Previously, buckling stability of viscoelastic structures have been particularly of interest for the application of steel columns at high temperatures due to fire, and polymer matrix composite materials in hygrothermal environments. When a viscoelastic structure is subjected to a force, the application of forces is responded by the instantaneous modulus of the material. As time makes progress, stress relaxation effects take place which cause the modulus to decline. This, in turn, decreases the critical buckling load of the structure which is a function of the *time-dependent modulus*. As soon as the critical buckling load is decreased to the level of applied load, the structure buckles.

The literature in the context of composite plates exhibiting some degree of anisotropy and viscoelasticity is reviewed here. Two approaches are available for solving the buckling problems. Firstly, is the viscoelasticity method which is also known as the *quasi-static* solution. Although variables are time-dependent it should be noted that the solution is different from dynamic buckling, in that inertia effects are neglected. The method utilizes Laplace or Laplace-Carson transformations to circumvent the integral equations in the governing viscoelastic differential equations by mapping them into regular multiplications.

The second method is the *quasi-elastic* solution. This approximation method ignores the stress variations with time and assumes that internal forces and moments are time-wise constant. By doing so, the time-varying viscoelastic properties can be directly substituted in the elastic solution. This method was first introduced by Schepary in 1965 [7] and it has been proved to be an effective assumption for various cases involving composite plates (see e.g. [8]).

2.2. Model

In this section, a novel buckling model is presented. As described in section 3, the problem is defined as an elastic orthotropic plate resting on general viscoelastic elements. A unit shear layer is introduced between the plate and foundation elements to increase the accuracy of the representation by producing an interaction between elements. This new foundation is called generalized viscoelastic foundation in the present study. By writing the force balance in the free body diagram of an infinitesimal element of the shear layer, the force that is being exerted on the plate ($F_{foundation}$) can be found:

$$F_{Foundation} = F_{visco} + G\left(w_{,xx} + w_{,yy}\right) \tag{1}$$

Where G is the modulus of the shear layer, w is the out-of-plane deformation of the plate, comma represents partial differentiation. Additionally, the force of viscoelastic elements is:

$$F_{visco} = -K * dw \equiv -\int_0^t K(t-\tau)\, dw(\tau) \tag{2}$$

Here, K is the equivalent of the stress relaxation function for the force-displacement relation. The negative sign demonstrates the resistive nature of the foundation response. Considering the small thickness to width or length ratio of the prepreg tow, Kirchhoff hypothesis shall be used for the plate.

Neglecting the in-plane displacements for the buckling problem, and simplifying for the Kirchhoff assumptions, the strain-displacement (*von Kármán*) relations can be found:

$$\varepsilon_{xx} = \frac{1}{2}\left(w_{0,x}\right)^2 - zw_{0,xx} \equiv \varepsilon^0_{xx} + z\varepsilon^1_{xx} \qquad \varepsilon_{yy} = \frac{1}{2}\left(w_{0,y}\right)^2 - zw_{0,yy} \equiv \varepsilon^0_{yy} + z\varepsilon^1_{yy}$$
$$\varepsilon_{xy} = \frac{1}{2}w_{0,x}w_{0,y} - zw_{0,xy} \equiv \varepsilon^0_{xy} + z\varepsilon^1_{xy} \qquad \varepsilon_{zz} = \varepsilon_{xz} = \varepsilon_{yz} = 0 \tag{3}$$

The buckling problem is formulated through the application of the quasi-static principle of virtual displacements. This principle states that:

$$\delta W_I + \delta W_E \equiv \delta W = 0 \tag{4}$$

The principle holds independent of the constitutive law used to describe the material properties. In this equation, the internal virtual work is $\delta W_I = \int_\Omega \sigma : \delta\varepsilon \, d\Omega$ where Ω is the volume of the plate; and δW_E is the virtual work of the external forces (i.e. foundation force in this case). Substituting the strains from Eq. 3 into the internal virtual works and integrating over the thickness (h) will introduce stress resultant terms, as a result of membrane strains (ε^0), and flexural stiffness-curvature terms resulted from the bending or flexural strains (ε^1).

$$\delta W_I = \int_A \begin{bmatrix} N_{xx}w_{0,x}\delta w_{0,x} + N_{yy}w_{0,y}\delta w_{0,y} + N_{xy}\left(w_{0,x}\delta w_{0,y} + w_{0,y}\delta w_{0,x}\right) + D_{11}w_{0,xx}\delta w_{0,xx} \\ +D_{12}\left(w_{0,xx}\delta w_{0,yy} + w_{0,yy}\delta w_{0,xx}\right) + D_{22}w_{0,yy}\delta w_{0,yy} + 4D_{66}w_{0,xy}\delta w_{0,xy} \end{bmatrix} dA \tag{5}$$

N_{ij} and D_{ij} respectively represent in-plane stress resultants and flexural laminate stiffness according to the classical laminate theory. In addition, using Eq. 2, the virtual work of external forces can be found.

$$\delta W_E = \int_A \left(K * dw \; \delta w_0 + Gw_{0,x}\delta w_{0,x} + Gw_{0,y}\delta w_{0,y}\right) dA \tag{6}$$

Eqs. 4, 5 and 6 together can fully define the problem.

The plate can be considered to be rectangular with a free edge (where the buckling occurs), two clamped edges and a free edge [3] (Fig. 2). A general axial load is applied to the plate, $N_{xx}(y) = P_0(1 - \alpha y/b)$. α Determines the load distribution, b is the tow width and P_0 determines the maximum value of the buckling load.

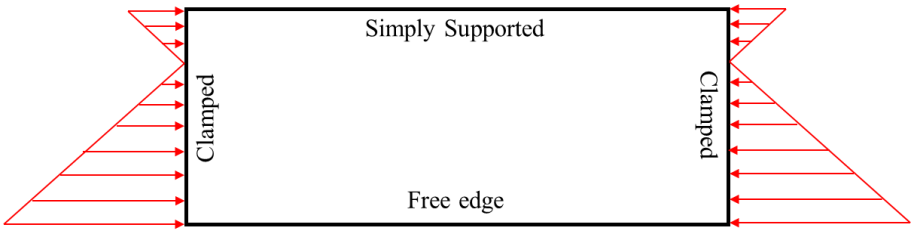

Figure 2. Boundary conditions.

Rayleigh-Ritz method is implemented to solve the governing equations. A complete series of linearly independent basis functions of variable amplitudes is normally required to represent the out-of-plane deformation of the plate. However, as demonstrated by Weaver (e.g. [9]), using appropriate one-term deformation functions that can effectively capture the overall form of the plate is also possible. A one-term displacement series has the distinct advantage over an infinite series in that an approximate *closed-form* solution becomes viable. The following shape functions are used:

$$u = \sum_{j=1}^{N} c_j(t)\varphi_j(x,y) \qquad \delta u = \sum_{i=1}^{N} \delta c_i(t)\varphi_i(x,y)$$
$$\varphi_j(x,y) = \left(1 - \frac{y}{b}\right)^{j+1}\left(1 - \cos\frac{2\pi m}{l}x\right) \tag{7}$$

In Eq. 7, *j* determines the buckling mode number. For the specific application of the present study, i.e. wrinkle formation, buckling always occurs in the first mode (*j=1*). After substituting Eq. 7 in Eq. 4, Laplace-Carson transformation is performed to map the asterisk operator of Eq. 2 into a multiplication that can be managed easily for continuing the Ritz solution. Subsequently, the Eigenvalue problem is solved.

$$\left([\tilde{R}(s)] - \widetilde{P_0}[B]\right)\{\tilde{c}_j(s)\} = \{0\} \tag{8}$$

Where *s* is the Laplace-Carson variable and tilde represents the transformed function. Additionally:

$$B_{ij} = \int_A \varphi_{j,x}\varphi_{i,x}\left(1 - \frac{\alpha y}{b}\right) dA \tag{9}$$

$$\widetilde{R_{ij}}(s) = \int_A \begin{bmatrix} D_{11}\varphi_{i,xx}\varphi_{j,xx} + D_{12}\left(\varphi_{j,yy}\varphi_{i,xx} + \varphi_{j,xx}\varphi_{i,yy}\right) + D_{22}\varphi_{j,yy}\varphi_{i,yy} + \\ 4D_{66}\varphi_{j,xy}\varphi_{i,xy} + G\varphi_{j,x}\varphi_{i,x} + G\varphi_{j,y}\varphi_{i,y} + \tilde{K}(s)\,\varphi_i\varphi_j \end{bmatrix} dA \tag{10}$$

Finally, the critical time-dependent buckling load can be obtained from Eq. 8:

$$P_{cr}(t) = \mathcal{L}^{-1}\left\{\frac{1}{s}\frac{[\widetilde{R(s)}]}{[B]}\right\} \tag{11}$$

Where $\mathcal{L}^{-1}$ is inverse Laplace transform.

3. Results and discussion

Various AFP trials were performed to better understand the wrinkle formation process [4]. The material used was 977-2/35-12K HTS-145 unidirectional prepreg which was characterized previously [3]. Fig. 3 shows the prepreg tow which was laid down with steering radius of 558.8 mm at two distinct times: immediately after deposition and about 60 seconds later. Clearly, the relaxation of interface takes place causing wrinkles to appear after a while.

(a)

(b)

Figure 3. An example of experimental trials: (a) $t = 0\ (sec)$; (b) t~60 (sec)

The mechanical properties of prepreg tow are presented in Table 1 and are used for the following calculations. The time-dependent critical buckling load is provided by equation 11. A general way of defining the viscoelastic mechanical properties is through the Prony series. The unknown parameters can be found by fitting the results to the experimental data.

$$K(t) = k_\infty + \sum_{i=1}^{n} k_i \exp(-t/\tau_i) \tag{12}$$

Where k_∞ is the long term modulus once the interface is fully relaxed, τ_i are the relaxation times and k_i are the elastic moduli in series with dashpots.

Table 1. Material properties.

E_1 (GPa)	E_2 (MPa)	G_{12} (MPa)	ν_{12}	h (mm)	b (mm)	α	G, Shear layer (N/m)
31	0.046	3.025	0.2	0.2	6.35	2	605

Fig. 4 shows the critical buckling load for various relaxation times. In a Maxwell model (one branch of $k\exp(-t/\tau)$), the relaxation time is defined as the ratio of viscosity over the branch's stiffness. Additionally, prepreg tack has been previously shown to be thermorheologically simple; ergo, follows the time temperature superposition [10]. Therefore, while the branch stiffness remains constant with increasing temperatures, viscosity drops, causing the decrease of relaxation time. On the other hand, increasing temperature decreases the storage modulus and, prior to the glass transition temperature, increases the loss modulus of the resin. Consequently, increasing temperature (so long as it does not initiate curing reactions) is imperative for establishing an intimate contact between the tool and prepreg, hence helps in having appropriate levels of tack. This study highlights that this could accompany decreased levels of relaxation time. *When* the wrinkles start to form, is critical in the manufacturing process, which is represented through the relaxation time in the present model. Further understanding the correlations and ultimately, modeling the parameters of the Prony series with respect to the AFP process parameters remain crucial objectives to be attained in the future studies.

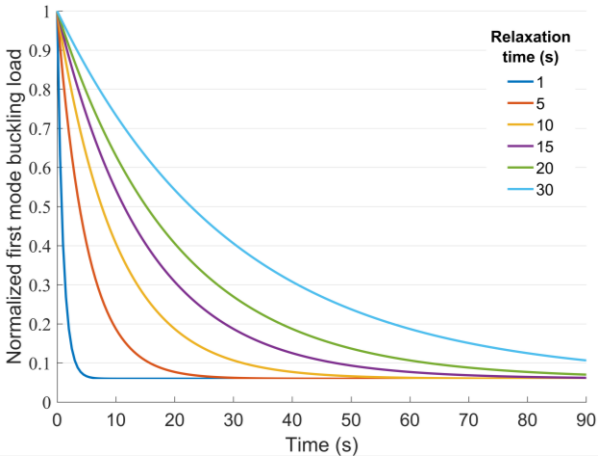

Figure 4. First mode buckling load for various relaxation times.

In the tow steering process, the induced load has a constant value which can be calculated. Using the Euler-Bernoulli beam theory, the prescribed curvature of the path shall be related to the induced load. If the induced load is greater than the instantaneous critical buckling load of the plate (see Fig. 4) the wrinkles will appear as soon as the prepreg tow is laid down on onto the tool surface. On the other hand, if the induced load is lower than the relaxed critical buckling load the wrinkled never occur and the steered tow will remain intact. When the induced load is between these two extreme cases, however, the viscoelastic effects will be dominant and wrinkles may appear as time makes progress. In this case, Eq. 11 can be solved for the length, in order to find how the wrinkle length grows with time.

4. Conclusions

Automated Fiber Placement has been increasingly used in the aerospace industry for the manufacturing of high-performance composite parts with high productivity and consistent part quality. Manufacturing of novel design philosophies such as variable stiffness panels which fully utilize the directionality of composites, has become possible using the AFP technology. Therefore, further optimization and development of both the manufacturing process and design of the parts require a better understanding of the limitations of the technology.

One of the major issues constraining the application of variable stiffness composites and lamination of complex parts is the defects that appear in prepreg tows during tow steering. Various defects including gaps and overlaps between the courses, wrinkles, and blisters appear in a ply. This study presents the effect of viscoelastic material properties that prepreg-tool interface exhibits on the formation of wrinkles. An example of experiments for the case where wrinkles appear with time is presented.

Different methodologies for describing viscoelasticity and solving time-dependent buckling problems involving viscoelastic materials are discussed. A novel buckling model for an orthotropic plate resting on a generalized viscoelastic Pasternak foundation is developed. Furthermore, the application of the developed model to the wrinkles that appear in the AFP process is discussed.

Acknowledgments

Financial support from the Natural Sciences and Engineering Research Council of Canada (NSERC) is gratefully acknowledged.

References

1. Dirk, H.-J.L., C. Ward, and K.D. Potter, *The engineering aspects of automated prepreg layup: History, present and future.* Composites Part B: Engineering, 2012. **43**(3): p. 997-1009.
2. Lozano, G.G., et al., *A review on design for manufacture of variable stiffness composite laminates.* Proceedings of the Institution of Mechanical Engineers, Part B: Journal of Engineering Manufacture, 2016. **230**(6): p. 981-992.
3. Belhaj, M. and M. Hojjati, *Wrinkle formation during steering in automated fiber placement: Modeling and experimental verification.* Journal of Reinforced Plastics and Composites, 2018: p. 0731684417752872.
4. Bakhshi, N. and M. Hojjati, *Simulating layup defects during tow steering in automated fiber placement.* Proceedings of The Canadian Society for Mechanical Engineering International Congress, CSME, 2018.
5. Kerr, A.D., *Elastic and Viscoelastic Foundation Models.* Journal of Applied Mechanics, 1964. **31**(3): p. 491-498.
6. Georgievskii, D., *Methods of investigation of boundary value problems in viscoelasticity theory.* Russian Journal of Mathematical Physics, 2007. **14**(3): p. 262-274.
7. Schapery, R.A., *A method of viscoelastic stress analysis using elastic solutions.* Journal of the Franklin Institute, 1965. **279**(4): p. 268-289.
8. Wilson, D.W. and J.R. Vinson, *Viscoelastic analysis of laminated plate buckling.* AIAA journal, 1984. **22**(7): p. 982-988.
9. Weaver, P. and J. Herencia. *Buckling of a flexurally anisotropic plate with one edge free*. in *48th AIAA/ASME/ASCE/AHS/ASC Structures, Structural Dynamics, and Materials Conference*. 2007.
10. Crossley, R.J., P.J. Schubel, and D.S.A. De Focatiis, *Time–temperature equivalence in the tack and dynamic stiffness of polymer prepreg and its application to automated composites manufacturing.* Composites Part A: Applied Science and Manufacturing, 2013. **52**: p. 126-133.